Optimization of plant-derived punicic acid synthesis in *Saccharomyces cerevisiae* by Ty retrotransposon-targeted random gene shuffling

Juli Wang, Guanqun Chen*

Department of Agricultural, Food and Nutritional Science, University of Alberta, Edmonton, Alberta, T6G 2P5, Canada.

*Corresponding author. Email: gc24@ualberta.ca. Phone: 780-492-3148.

Abstract

Producing high-value plant-derived unusual fatty acids in microorganisms via synthetic biology is attractive, but increasing their contents through rational step-by-step gene stacking is challenging. Using *Saccharomyces cerevisiae* and pomegranate-derived punicic acid (PuA) as representatives, an efficient, result-driven gene shuffling strategy was developed to facilitate the production of value-added plant lipids. By targeting yeast Ty retrotransposon regions, candidate genes related to PuA production were directly shuffled within the yeast genome to create recombinant libraries. Subsequent screening and bioprocess optimization led to a recombinant yeast strain with 26.7% of total fatty acids as PuA through neosynthesis. Further analyses revealed that the strain hosts multiple genes, contains over 22% PuA in the storage lipid triacylglycerol, and has substantial changes in its lipidome. Overall, this work provided an efficient strategy for improving PuA content in yeast, which could be adopted to engineer microorganisms for the production of other high-value plant-derived fatty acids and bioproducts.

Keywords

punicic acid, unusual fatty acid, pomegranate, metabolic engineering, *Saccharomyces cerevisiae*, Ty retrotransposon.

1. Introduction

Some plant species have remarkable abilities in synthesizing unusual fatty acids (UFAs), which possess distinct chemical structures and higher values compared to common fatty acids (Cahoon and Li-Beisson, 2020), but most of these plants are not ideal crops for large-scale agriculture. Therefore, it is attractive to produce plant-derived UFAs in engineered industrial microorganisms such as yeast, as they can be cultured in a controlled bioreactor with short production cycles and greatly reduce arable land requirements. However, given the complexity of the pathways involved in plant-derived UFA synthesis and accumulation, it is time-consuming to test each gene separately to achieve pathway functionality, and even more challenging to efficiently obtain the best gene combination for their transgenic production. Thus, a more effective process is needed to efficiently generate robust microorganism strains for the production of plant-derived UFAs.

Pomegranate (*Punica granatum*) derived punicic acid (PuA; 18: $3\Delta^{9cis,11trans,13cis}$) is a typical conjugated fatty acid and a representative plant-derived UFA (Paul and Radhakrishnan, 2020). The three conjugated double bonds in PuA offer a wide range of health benefits, as well as potential applications in the oleochemical industry (Holic et al., 2018; Shockey et al., 2016). Given the emerging applications of PuA in the nutraceutical and chemical industries, its potential market is expected to experience significant growth in the coming years (Holic et al., 2018; Paul and Radhakrishnan, 2020). As a result, the market price of pomegranate seed oil, depending on

its purity, has been reported to be relatively high (Holic et al., 2018; Paul and Radhakrishnan, 2020; Urbanikova et al., 2023). However, growing pomegranate for large-scale PuA production has significant challenges, such as a low seed-to-fruit ratio and low oil yield compared to oilseed crops (Fadavi et al., 2006; Lansky and Newman, 2007). Although initial efforts have been made to generate PuA-producing plants via genetic engineering, their PuA contents were still quite low (Mietkiewska et al., 2014; Xu et al., 2020b).

Given the constraints faced by PuA-producing transgenic plants, such as lengthy breeding procedures, susceptibility to climate change, and significant arable space requirements, microorganisms emerge as a promising alternative. For this reason, we previously engineered baker's yeast (*Saccharomyces cerevisiae*), a Generally Recognized as Safe (GRAS) microorganism, to produce PuA (Wang et al., 2021). In pomegranate, bifunctional acyl lipid desaturase and conjugase (PgFADX) converts the common fatty acid linoleic acid (LA) on the *sn*-2 position of phosphatidylcholine (PC) to PuA (Iwabuchi et al., 2003). However, the coexpression of the genes encoding PgFADX and LA-producing pomegranate Δ12 acyl lipid desaturase (PgFAD2) only led to 0.3% PuA in *S. cerevisiae* (Wang et al., 2021). Since *S. cerevisiae* is a conventional yeast with limited lipid content (He et al., 2018), this initial low level of PuA could be attributed to inefficiencies in lipid biosynthesis. However, a recent study revealed that PuA production was also fairly low in *Yarrowia lipolytica*, which is a well-studied oleaginous yeast (Urbanikova et al., 2023). These results suggested that the lipid-accumulating capabilities of different yeast platforms may not be the dominant factor leading to the low contents of PuA.

In addition, many biosynthetic pathways upstream and downstream of the PgFADX-catalyzed reaction in transgenic hosts may not synergize effectively with each other for efficient PuA production. For instance, the enrichment of UFAs in plant oils involves a series of enzymatic reactions that occur in developing seeds (Cahoon and Li-Beisson, 2020; Napier, 2007). These reactions form the acyl-editing and triacylglycerol (TAG) assembly network, which dominates the flow of UFAs from polar lipid (PL) into TAG for their stable storage in lipid droplets (Fig.1A). Given the presence of this network, the UFA levels in the seed TAG of natural producers are significantly higher than in engineered transgenic hosts (Kaufman and Wiesman, 2007; Khoddami et al., 2014; Mietkiewska et al., 2014; Paul and Radhakrishnan, 2020; Xu et al., 2020b). In line with this, while PuA is the major fatty acid species in pomegranate seed TAG, engineered transgenic *Brassica napus* and *Arabidopsis thaliana* only accumulate 6.6% and 10.6% of PuA in seed TAG fractions, respectively (Mietkiewska et al., 2014; Xu et al., 2020b).

The objectives of this study were to develop an efficient, results-driven approach for testing the performance of pathway genes and to enhance the accumulation of value-added PuA in recombinant *S. cerevisiae* strains through metabolic engineering. By targeting the locations of yeast Ty retrotransposon, we directly shuffled genes that potentially contribute to PuA synthesis on yeast genome and generated a recombinant yeast library with various contents of PuA. Subsequent screening of the library as well as preliminary optimization led to a recombinant yeast strain with 26.7% of total fatty acids as PuA without the need for LA precursor feeding. In shake flask cultivation, the PuA titer reached 425 mg/L. Furthermore, lipidomic and positional analyses revealed substantial changes in the yeast lipidome resulting from PuA synthesis, where PuA comprised over 22% of total fatty acids in the TAG fraction of yeast single-cell oil. To the

best of our knowledge, the PuA content and titer are the highest achieved in engineered *S. cerevisiae*, demonstrating the value of the strategy used in this study, which can be modified and applied for producing other high-value UFAs and bioproducts in yeast cells.

2. Materials and methods

2.1. Strains, genes, and plasmids

All strains used in this study are listed in Table S1. In brief, *Escherichia coli* DH5α was used for routine plasmid construction and preparation. *S. cerevisiae* BY4741- *snf2Δ* obtained from the Euroscarf collection was used as the starting strain in this study. *S. cerevisiae* H1246 quadruple mutant lacking lipid biosynthetic ability was used to test the performance of pomegranate genes. Yeast transformations were performed using the traditional lithium acetate and PEG3350 method as described previously (Gietz and Schiestl, 2007). To obtain the template for cloning TAG assembly and acyl-editing genes from *P. granatum*, total RNA was isolated from *P. granatum* tissues using the Spectrum Plant Total RNA Kit (Sigma-Aldrich, Oakville, Canada) and cDNA was synthesized using the SuperScript IV first-strand cDNA synthesis kit (Invitrogen, Carlsbad, USA). Putative sequences were obtained by performing an NCBI Basic Local Alignment Search Tool (BLAST) search against the online draft genome of *P. granatum* (Luo et al., 2020).

The target Ty retrotransposon region was analyzed based on the S288C reference genome from the *Saccharomyces* Genome Database (SGD) (http://www.yeastgenome.org/). Similarity and identity searches for target sequences in Ty retrotransposons were conducted using BLAST. Plasmids providing donor DNA were derived from pUC19. Four components, including upstream homology sequence, gene expression cassette, selection marker with truncated

promoter region (*leu2*, *his3*, and *ura3* for round 1, 2, and 3 integrations, respectively), and downstream homology sequence were inserted. To release donor DNAs from the pUC19 backbone, either PCR or double digestion of SmaI sites flanking the donor DNA was conducted. For different genes, 500 fmol of each donor DNA were pooled together. To facilitate integration, CRISPR-Cas9 expression vectors (based on plasmid pCRCT, obtained from Addgene, plasmid #60621) targeting different locations on Ty retrotransposons were constructed and co-transformed into yeast cells with donor DNA (Bao et al., 2015). Three 20bp sequences that are adjacent to the PAM sites that occur frequently in the respective target regions were selected as the spacer sequences for delivering crRNA (Table S2). These sequences were ordered as single-stranded, complementary oligos and annealed to obtain double-stranded DNAs. By adding homology arms, these sequences were inserted between two Eco31I restriction sites on the pCRCT plasmid.

2.2. Culture conditions and optimization

For plasmid construction and preparation, *E. coli* was cultured at 37 °C in the Luria-Bertani (LB) medium with shaking at 225 rpm. To sustain the plasmids in *E. coli*, 100 mg/L ampicillin was applied. For testing PuA accumulation in shake flask cultivation, individual colonies of transformed yeast cells were first grown in 5 mL yeast nitrogen base (YNB) supplemented with an appropriate amino acid drop-out mix and 2% glucose for 24 h at 30 °C with shaking. Seed cultures were then inoculated into 1 L shake flasks containing 60 mL synthetic complete medium (6.7 g/L YNB, 2 g/L synthetic complete supplement mixture of amino acids, and 6% glucose). The inoculum for PuA production experiments was grown for 72h at 20 °C or 30 °C, using an incubated shaker with a shaking speed of 250 rpm. For culture condition optimization, the Box–

Behnken design was employed for response surface methodology. The factors considered for optimization were examined at three levels (6%, 10.5%, and 15% for glucose; 5.3, 6.5, and 7.6 for initial pH; 0.2, 0.6, and 1 for initial OD_{600}). The two responses considered for analysis were PuA content (% of total fatty acids) and PuA titer (mg/L). Based on the results, second-order polynomial equations were fitted to predict the optimal points within experimental constraints (Table S3).

2.3. Preparation of plant oil hydrolysate and fatty acid feeding

Preparation of free fatty acids from pomegranate seed oil was conducted using chemical hydrolysis (Salimon et al., 2011). In brief, 50 g of pomegranate seed oil was mixed with 12 g potassium hydroxide, 117 mL pure ethanol, and 35 mL H_2O in a shake flask flushed with nitrogen. The butylated hydroxytoluene (BHT) solution was added to the mixture to protect PuA. The reactor was then sealed and maintained at 50 °C with constant shaking. After 1 h of incubation, removal of the unsaponifiable matter was performed three times by mixing 100 mL of distilled water and 100 mL of hexane. Free fatty acids were extracted with 100 mL hexane and dried over anhydrous sodium sulfate. The solvent was then removed under vacuum to obtain pomegranate oil hydrolysate. When fatty acid feeding was required, 0.03% v/v ethanol dissolved LA or pomegranate oil hydrolysate was supplemented to the culture medium along with 0.2% non-ionic surfactant NP-40 (TERGITOL™ solution) for even distribution of fatty acid in the aqueous medium.

2.4. Nile red staining of neutral lipids in yeast

Nile red fluorescence detection was conducted as described previously (Pan et al., 2013). Briefly, 100 µl aliquots of the yeast cell suspension were transferred to a 96-well dark flat-bottom plate. Background fluorescence was measured using a Synergy H4 Hybrid multimode microplate reader (Biotek Instrument, Inc.) with emission and excitation filters set to 485 and 538 nm, respectively. A newly prepared methanolic Nile red solution (0.1 mg/mL) was added, and the second fluorescence intensity was measured. The Nile Red values were calculated based on the change in fluorescence over OD_{600} ($\Delta F/OD_{600}$).

2.5. Lipid extraction and separation of lipid class using thin-layer chromatography

Before lipid extraction, yeast biomass was harvested from liquid culture via centrifugation. The supernatant was then removed and 800 µL of a cold lipid extraction mixture comprising chloroform and isopropanol (2:1, v/v) was added, along with glass beads (0.5mm) and BHT at a final concentration of 0.01% (Garaiova et al., 2017; Mietkiewska et al., 2014). Subsequently, cellular disruption was achieved through three cycles of bead beating (1-minute duration each) using a Biospec bead beater (Biospec, Bartlesville, OK), with 2-minute cooling on ice between each cycle. The extraction procedure was repeated twice for each sample. The collective organic phase, containing both PL and TAG, was dried under nitrogen and resuspended in 200 µl chloroform. For lipid class analysis, the lipid extracted from each sample was separated using thin layer chromatography (TLC) with silica gel-coated plates (0.25 mm Silica gel, DCFertigplatten, Macherey-Nagel, Germany). The TLC plates were developed using a solvent mixture comprising hexane/diethyl ether/acetic acid (in a 70:30:1 ratio) (Xu et al., 2020b). Lipid fractions on the TLC plate were visualized via 0.05% primulin staining under UV light. Bands

corresponding to target lipid fractions were scraped, extracted, derivatized, and subsequently analyzed.

2.6. Positional analysis of triacylglycerol and polar lipids

The fatty acid distribution between *sn*-2 and *sn*-1/3 TAG was analyzed using previously described enzymatic reactions (Luddy et al., 1964; Xu et al., 2020b). Briefly, after TLC separation, TAG was recovered from the silica gel, and dried under nitrogen. Subsequently, 1 mL Tris-HCl buffer (1 mM, pH 8.0), 100 μL 2.2% $CaCl_2$, and 250 μL 0.1% deoxycholate was added. Each mixture was vortexed for 2 minutes and sonicated for 60 seconds to emulsify the lipid. The mixture was pre-warmed in a water bath at 40 °C for 30 s, and then 20 mg pancreatic lipase (pancreatic lipase type II, Sigma) was added to initiate hydrolysis. The mixture was further incubated for 3 min at 40 °C, and the reaction was terminated by adding 500 μL of 6 M HCl. The resulting lipids, containing unreacted TAG, diacylglycerol (DAG), monoacylglycerol (MAG), and free fatty acids, were extracted twice with 3 mL of diethyl ether and then separated using TLC. The *sn*-2 MAG was subsequently analyzed.

The positional analysis of PL was performed by cleaving the fatty acids at the *sn*-1 position of PL using phospholipase A_1 (Vikbjerg et al., 2006; Xu et al., 2020b). In brief, phospholipase A_1 was first mixed with water in a 1:4 (v/v) ratio. PL was recovered from the silica gel and dissolved in 2 mL of diethyl ether, and 1 mL of phospholipase A_1 (Sigma) solution was added to initiate hydrolysis. The mixture was then vortexed at maximum speed for 5 min and the reaction was terminated by evaporation of diethyl ether under nitrogen. The hydrolyzed lipids were extracted and separated by TLC, and cleaved fatty acids were subsequently analyzed.

2.7. Lipid transmethylation, analysis and lipidomic profiling

To prepare fatty acid methyl esters (FAMEs), transmethylation was carried out via a base-catalyzed method using 1 mL of 5% sodium methoxide dissolved in methanol (Garaiova et al., 2017; Mietkiewska et al., 2014). After incubation at 30 °C for 1 h, the reaction was stopped by adding 1.5 mL of 0.9% (w/v) sodium chloride solution. FAMEs were then extracted with 1 mL of hexane. Subsequently, the FAMEs were analyzed on an Agilent 6890N Gas Chromatograph equipped with a 5975 inert XL Mass Selective Detector and Flame Ionization Detector (Agilent Technologies) using a method described in our previous study (Mietkiewska et al., 2014; Xu et al., 2020b). Briefly, FAMEs were separated on a capillary column DB23 (30 222 m×0.25 mm×0.25 µm, Agilent Technologies, Wilmington, DE, USA) using the following program: 2:1 split ratio, 1 µL injection. 4 min at 165 °C, then increased to 180 °C (10 °C/ min) and held for 5 min, and increased to 230 °C and held for 5 min. The lipidomic analyses described in this work were performed at the Kansas Lipidomic Research Center analytical laboratory. The lipidome of four chosen yeast strains was investigated. In the analyses, four cultures of each yeast strain were used as replicates. All biological replicates were cultured under the same conditions, and samples were collected after 96 h.

3. Results

3.1. Functional validation of pomegranate genes in yeast and the construction of PgFADX variants

Acyl-editing and TAG assembly are important biochemical processes for fatty acid modification and accumulation in plants (Fig. 1A), where specialized enzymes collaborate to edit and

exchange specific acyl groups, redistributing them across various lipid pools and enriching the target fatty acid within the TAG fraction (Cahoon and Li-Beisson, 2020). Since most pomegranate enzymes involved in this process have not been fully studied, we first conducted the identification and isolation of the genes encoding these enzymes. As listed in Table S4, we obtained genes encoding three pomegranate diacylglycerol acyltransferase 2 (DGAT2), three phospholipid: diacylglycerol acyltransferase (PDAT), and one of each of the following enzymes: diacylglycerol acyltransferase 1 (DGAT1), phosphatidylcholine: diacylglycerol cholinephosphotransferase (PDCT), lysophosphatidylcholine acyltransferase (LPCAT), glycerol-3-phosphate acyltransferase 9 (GPAT9), lysophosphatidic acid acyltransferase 2 (LPAT2), phospholipase A_2 (PLA_2), phospholipase C (PLC), and long-chain acyl-CoA synthetase 8 (LACS8).

Since DGAT and PDAT catalyze the crucial final committed step in plant TAG biosynthesis (Chen et al., 2022), we tested the functions of the identified pomegranate DGAT and PDAT in yeast. The genes encoding PgDGAT1, PgDGAT2.a, PgDGAT2.b, PgDGAT2.c, PgPDAT.a, PgPDAT.b, and PgPDAT.c were transformed into *S. cerevisiae* H1246, a quadruple mutant strain incapable of synthesizing storage lipids including TAG (Sandager et al., 2002). As shown in Fig.1B, yeast strains expressing *PgDGAT1*, *PgDGAT2.a*, and *PgDGAT2.b*, respectively, restored TAG synthesis ability. Since pomegranate oil contains a high level of PuA, it is plausible to assume that pomegranate-derived TAG assembly enzymes may evolved a preference for PuA-containing substrate. To test this hypothesis, we fed the recombinant yeast strains with pomegranate oil hydrolysate. The results indicated that the strains hosting pomegranate PgDGAT2.c and PgPDAT.a, respectively, could incorporate pomegranate oil hydrolysate to

TAG (Fig.1C). Specifically, the expression of *PgDGAT2.c* led to PuA comprising 20% of the total fatty acids in TAG, suggesting a potential substrate preference for this conjugated fatty acid (Fig.1D).

Moreover, various protein fusions have been used to enhance enzyme performance in metabolic engineering efforts (Xu et al., 2020a; Andre et al., 2013). For instance, our previous study revealed that fusing algal DGAT with an acyl-CoA binding protein, which attracts the substrates for DGAT-catalyzed reactions, led to a kinetic improvement of the enzyme (Xu et al., 2020a). Additionally, protein fusion can also be used to remove harmful byproducts, as shown in a previous study where combining aldehyde deformylating oxygenase with catalase alleviated inhibition from H_2O_2 accumulation (Andre et al., 2013). In pomegranate, PgFADX is responsible for converting the common fatty acid LA to PuA through a desaturase-like reaction, which requires an electron donor, molecular oxygen, and PC as the acyl carrier (Yazawa et al., 2010; Cerone and Smith, 2022; Iwabuchi et al., 2003). In addition, H_2O_2 may also inhibit the activity of desaturase-like enzymes (Browse and Slack, 1981). Therefore, selected genes encoding the PC-binding protein (SCP2), oxygen carrier-protein, soluble domain of the electron transporter cytochrome b5 (CB5SD), and catalase were linked with PgFADX, respectively. The expression cassettes containing these fusions were transformed into BY4741 *snf2Δ* mutant, which exhibited an elevated level of fatty acid synthesis (Kamisaka et al., 2006). As shown in Fig. 1E, except for the fusion with catalase, all other PgFADX variants showed a slight increase in the PuA level. In addition, yeast SNF1 (sucrose non-fermenting 1) is a protein kinase and master regulator that plays a critical role in regulating yeast energy metabolism and glucose homeostasis (Usaite et al., 2009), and its deletion could lead to enhanced lipid biosynthesis in yeast cells (Seip et al., 2013).

Therefore, we also constructed a BY4741 *snf2Δ snf1Δ* double knockout mutant by replacing the *snf1* gene with an *AtSCP2-PgFADX* expression cassette. As shown in Fig. 1E, when *AtCB5SD-PgFADX* was expressed in this strain mutant background, PuA accounted for 6% of the total fatty acids.

3.2. Improved bioconversion from linoleic acid to punicic acid in yeast strains constructed by Ty retrotransposon-targeted integration

The above results were obtained with the plasmid-based gene expression approach, which is less stable without selective pressure and may lead to lower expression levels as well as *in vivo* enzyme concentrations (Karim et al., 2013; Lian et al., 2016). Therefore, following these experiments on gene characterization, a workflow was developed for effective integration and testing of UFA accumulation-associated genes directly on the yeast genome. The yeast Ty retrotransposon elements were chosen as the locus for integration, and CRISPR-Cas9 systems were used to facilitate the process. *S. cerevisiae* genome contains a large number of Ty retrotransposon elements (Curcio et al., 2015). Since they do not participate in yeast metabolism, the integration of genes into these regions will lead to higher copy numbers with lower interference with cellular fitness (Kato et al., 2013; Shi et al., 2016). Therefore, sequence analysis of yeast Ty retrotransposon and its long terminal repeats (delta sequence) was conducted first. Based on the result, *YERCdelta20* (Table S5), *YDRWdelta23* (Table S6), and *TyA Gag* gene (Table S7) were chosen as the targets for gene shuffling due to their high similarity with other analyzed sequences. The proposed workflow and designed donor DNA structure are illustrated in Fig. 2A and Fig. 2B, respectively. Various donor DNAs containing expression cassettes were constructed by flanking candidate genes with homology arms targeting yeast Ty retrotransposon.

Selection markers with defective promoter regions were also included to enhance the probability of obtaining positive transformations with higher gene copy numbers. Next, the cassettes were co-transformed into yeast cells with the CRISPR-Cas9 system. Various transformants were then individually cultured in small tubes and tested for their intracellular lipid and PuA levels. Based on our previous results (Wang et al., 2021), 0.03% LA was added to the liquid culture in the first and second round screening as the fatty acid precursor but was omitted in the third-round screening, which aimed for PuA neosynthesis.

Given the critical role of PgFADX, we integrated the *AtCB5SD-PgFADX* expression cassette into the BY4741 *snf2Δ snf1Δ* double knockout mutant during the first round of yeast Ty retrotransposon-targeted integration and subsequently screened 360 strains. With LA feeding, PuA accumulation was detected in all transformants (Fig. 3A). Only a small number of yeast strains (10%) accumulated less than 6% of total fatty acids as PuA. The majority of the strains (84%) accumulated 6%-10% of PuA, and 6% strains accumulated over 10% of PuA. The PuA content in the best strain, designated as CARIA266, reached nearly 11%. To further probe the performance of CARIA266, we conducted a growth analysis of this strain in shake flasks under different culturing temperatures. As shown in Fig. 3B, CARIA266 maintained a high PuA level of up to 12.6% at 96 h of cultivation under 20 °C. Compared to 30 °C, CARIA266 accumulated more monounsaturated fatty acid (MFA) under 20 °C, and the level of PuA gradually increased during the 4-day periods. When cultured under 30 °C, the level of PuA was relatively stable and slightly lower than the level obtained under 20 °C. The highest titer of PuA was 69 mg/L on day 5.

Notably, CARIA266 also accumulated a high content of LA, which was not converted to PuA (Fig. 3B). Even though the PuA level in yeast strains obtained by Ty retrotransposon-targeted integration was significantly higher than those generated via the plasmid-based approach, the unexpected buildup of LA indicated that this fatty acid precursor was not efficiently edited, and the native TAG synthesis in yeast may not favor PuA accumulation. One possible cause was the lack of specialized enzymes for acyl-editing and TAG assembly of PuA (Fig. 1A). Therefore, the round two Ty retrotransposon-targeted random gene shuffling focused on the introduction of those enzymes from pomegranate. Since PgDGAT1, PgDGAT2a, PgDGAT2b, PgDGAT2c, and PgPDAT.a could restore TAG synthesis in yeast H1246 (Fig. 1B and 1C), their encoding genes along with *PgPDCT*, *PgLPCAT*, *PgGPAT9*, *PgLPAT2*, *PgPLA*$_2$, *PgPLC*, and *PgLACS8* were selected as the candidates.

All these donor DNAs were pooled together and co-transformed into CARIA266 with *YDRWdelta23*-targeting CRISPR-Cas9, and the transformants were cultured in the presence of 0.03% LA. Subsequently, in the 792 screened strains, 70% of them produced 8%-12% of total fatty acids as PuA and 7% accumulated PuA higher than 12% of total fatty acids (Fig. 3C). Compared to the first-round integration (Fig. 3A), the average amount of the PuA from round two strains was higher (Fig. 3C), indicating the enhanced production of PuA from additional gene combination. The majority of the population (96%) also had higher Nile red fluorescence, suggesting the improvement in neutral lipid accumulation caused by the pomegranate acyl-editing and TAG assembly enzymes. When the best strain, designated as CARIB650, was cultured in the shake flask under 20 °C, it accumulated 18% of total fatty acids as PuA, with the highest PuA titer of 94 mg/L (Fig. 3D). Compared to CARIA266, the content of LA in

CARIB650 on day 4 significantly dropped by 25%, indicating an improved conversion rate of this fatty acid precursor.

3.3. High-level neosynthesis of PuA in yeast cells using Ty retrotransposon-targeted random gene integration and culture condition optimization

The above results were obtained by bioconversion of manually fed LA precursor to PuA. Considering the higher costs and the need for consistent quality of precursors required by the bioconversion method, neosynthesis might represent a more advantageous choice. Therefore, the third round of integration was conducted to reconstitute and increase LA precursor supply *in vivo*. Codon-optimized donor DNAs encoding PuA-producing AtCB5SD-PgFADX, LA-producing PgFAD2, MFA-producing *Puccinia graminis* acyl-CoA desaturase (PgOLE1), and C18 fatty acid-producing *Rattus norvegicus* fatty acid elongase (RnELO2) (Table S8) were selected as the candidates for integrating into CARIB650. In total, 600 strains were screened without LA feeding. Via neosynthesis, 3% of the strains produced 10%-14% PuA and 0.8% produced PuA higher than 14% of total fatty acids (Fig. 3E). In this round of gene shuffling, 80% of the strains only produced 1%-2% PuA, which was possibly caused by the lack of *PgFAD2* integration. In shake flask cultivation, the best strain (CARIC568) could accumulate 18% PuA (102 mg/L) under 20 °C in 4 days without LA feeding (Fig. 3F). Taken together, 1752 yeast transformants were screened in three rounds using the workflow generated in this study. The PuA content and product titer have been improved significantly, and the content of total unsaturated fatty acid was increased from 80% (with LA feeding) in CARIA266 to 90% in CARIC568 (without LA feeding).

Subsequently, on the level of shake flask culture, a response surface methodology using a multifactorial Box-Behnken design was employed for culture condition optimization to explore the potential of CARIC568 in PuA production. As detailed in Table S3, the chosen variables including carbon, initial pH, and initial OD_{600} were varied at three levels. Results revealed carbon source level and initial pH were the most significant factors affecting PuA content and production in CARIC568 (Fig. 4A, 4B, and Fig. S1, S2). Next, second-order polynomial equations were fitted to the experimental results to predict the optimal points within experimental constraints (Table S3), which led to optimized conditions including 12% glucose, pH 7.04, and an initial OD_{600} of 0.72. A verification experiment was then carried out to determine the accuracy of the prediction. Following 120 h of incubation in this optimized condition, CARIC568 produced 425 mg/L PuA (Table 1). The lipid content reached 15.5% of dry cell weight, with PuA accounting for 26.7% of total fatty acids. To the best of our knowledge, this is the highest content and titer reported to date for PuA production in *S. cerevisiae*. Subsequent analysis of genomic DNA revealed that CARIC568 hosted *AtCB5SD-PgFADX* as well as *PgPDCT*, *PgLPCAT*, *PgDGAT2.c*, *PgFAD2* and *RnELO2*.

3.4. Lipidomic analysis revealed substantial changes in yeast lipidomes

To reveal how the lipid profile was influenced by Ty retrotransposon-targeted random gene shuffling, and to assess the impact of varying levels of PuA accumulation, extensive lipid analysis was conducted. This analysis encompassed four groups of samples across three strains, which exhibited low to high amounts of PuA. The conditions tested were as follows: CARIA266 and CARIC568 cultured without LA feeding, and CARIA266 and CARIB650 cultured with 0.03% LA feeding. As shown in Fig. 4C and 4D, when LA was omitted in the culture medium, the PuA

level in CARIA266 was relatively low. When LA was available, CARIA266 accumulated 7.8% and 51% of TAG as PuA and LA, respectively. After transforming pomegranate acyl-editing and TAG assembly genes to the genome, CARIB650 accumulated 15% PuA in TAG, representing a 92% increase over CARIA266. Meanwhile, the content of LA in both TAG and PL fractions was lowered in CARIB650. By synthesizing LA directly on PC, CARIC568 accumulated the highest PuA (22.4%) and the lowest LA (34.4%) in TAG fraction compared to other strains.

Subsequently, positional analysis of TAG was conducted, and the results revealed that, in CARIA266 with LA feeding, the *sn*-2 position of TAG contained 44.3% LA and 6.3% PuA (Fig. 4E). After the second round of integration, the LA content of CARIB650 at the *sn*-2 position of TAG was decreased by 19% whereas PuA was increased by 81.7%. In terms of CARIC568, PuA accounted for 14.5% of the fatty acids at the *sn*-2 position of TAG (Fig. 4E) and 26.3% of the fatty acids at the *sn*-1/3 position of TAG (Fig. 4G), suggesting a slight preference for enriching PuA at the *sn*-1/3 position in this strain. Positional analysis of PL indicated that the *sn*-1 position generally contained relatively lower levels of PuA (Fig. 4F). In contrast, PuA accounted for 21.7% (CARIA266+LA), 25.3% (CARIB650+LA), and 47.1% (CARIC568) of the fatty acids at the *sn*-2 position of PL (Fig. 4H), which is consistent with the widely held opinion that the *sn*-2 position of PL is the location for acyl-editing.

To further examine the impact of PuA production on yeast lipid profile, a lipidomic analysis was conducted. The principal components analysis (PCA) revealed a clear distinction between the four lipidomes (Fig. S3). The distance between the final strain CARIC568 and starting strain CARIA266 on the PCA plot indicated significant alterations in the yeast lipidome as a result of

genetic modifications made by Ty retrotransposon-targeted integration. The TAG species in yeast lipidomes were separated into saturated fatty acid (SFA)-containing TAG, MFA-containing TAG, and polyunsaturated fatty acid (PUFA)-containing TAG. Heatmaps displaying the relative abundance of different TAG species are shown separately in Fig. 5 using a color scale. In CARIA266, the overall content of TAG containing SFA was noticeably greater (Fig. 5A). Compared with the CARIC568, CARIA266 accumulated more TAG with shorter chain SFA, such as TAG (50:2_16:0). In terms of MFA-containing TAG, CARIA266 accumulated a higher content of C16:1-containing TAG, and the overall saturation degree of CARIA266 TAG was higher (Fig. 5B).

As seen in Fig. 5C, the content of C18:2-containing TAG was relatively high in CARIA266+LA and CARIB650+LA as a result of exogenously added LA. In this regard, CARIB650 had a lower level of C18:2-containing TAG than CARIA266+LA, indicating the positive effects of pomegranate TAG assembly and acyl-editing genes. Since *S. cerevisiae* does not naturally accumulate C18:3 fatty acids (He et al., 2018), the C18:3 detected in the TAG fraction reflected the content of PuA. CARIC568 generated the highest content of PuA-containing TAG species, led by TAG (54:6_18:3) and TAG (54:5_18:3) (Fig. 5C). Compared to the other three lipidomes, CARIC568 had a significantly higher level of TAG species with high unsaturation degree (5-8 double bonds in total). However, in contrast to pomegranate seed oil, where the majority of PuA incorporated into TAG occupies all three positions of the glycerol backbone (Holic et al., 2018), the lack of TAG (54:9) in the top-ranking TAG species in all yeast lipidomes suggested that the PuA product was still primarily found at a single or double position of TAG glycerol backbone.

The tested yeast samples contained a variety of PL, including PC, lysophosphatidylcholine (LPC), lysophosphatidylethanolamine (LPE), phosphatidylserine (PS), phosphatidylethanolamine (PE), phosphatidylglycerol (PG), phosphatidylinositol (PI), and phosphatidic acid (PA) (Fig. 5D). In CARIA266, CARIA266+LA, CARIB650+LA, and CARIC568, the most abundant PL species are PE (34:2), PI (36:2), PC (36:4), and PC (36:5), respectively. A substantial up-regulation of unsaturation degree was observed across major PL species, such as PC (36:5), PC (36:6), PI (36:3), PI (36:6), PE (36:5), and PS (36:4), in response to increasing PuA production.

The comparison of differentially expressed lipids between various strains was shown in the volcano maps (Fig. 5). When exogenous LA was made accessible to CARIA266, TAG accounted for 60% of the up-regulated lipid species with C18:2-containing lipids being the majority (Fig. 5E). After the second-round integration, 82 lipid species and 45 lipid species were up- and down-regulated, respectively, with TAG accounting for 50%-78% of them (Fig. 5F). By switching PuA production from bioconversion to neosynthesis, 34 TAG and 25 PL species were up-regulated, whereas 47 TAG and 20 PL species with saturated acyl chains were down-regulated (Fig. 5G). When comparing the final strain CARIC568 with the starting strain CARIA266, significant changes in lipid species were observed. TAG accounted for 55% of both up- and down-regulated lipids (Fig. 5H). Most up-regulated lipids had more than four double bonds, whereas the down-regulated lipids consisted of shorter acyl chains with fewer double bonds (Fig. 5H).

4. Discussion

So far, the exact roles of enzymes involved in plant UFA synthesis, accumulation, and regulation are yet to be fully elucidated. Individually determining the functions and optimal expression levels of these proteins in plant or microbial hosts adds to the challenge of developing an efficient platform for the heterologous production of UFA. Instead of using traditional gene stacking strategies, where the exact gene candidates, combinations, and approximate ratios are designed before the experiment, the approach developed in this study randomly combined and integrated potentially necessary pathway genes into the yeast genome using CRISPR-Cas9, resulting in a pool of transformants. Subsequent screening of the yeast colonies identified a strain (CARIC568) with high PuA content and a gene combination conducive to PuA accumulation. This method may shed light on the production of other plant-derived UFAs in microorganisms.

In addition to the results-driven approach designed in this study, it would be interesting to further optimize other aspects for better performance. Although *S. cerevisiae* has been extensively used as a model microorganism to study plant enzymes, some plant-derived enzymes might accumulate poorly in yeast cells (Pan et al., 2013). This could potentially account for the variability in the results of the TAG synthesis complementation assays conducted in this study (Fig. 1B and 1C). In addition, the stability and turnover rate of PgFADX might also play a role in the process of PuA production. For instance, a previous study showed the N-terminal sequences of plant fatty acid desaturase confer a rapid degradation of the protein (Khuu et al., 2011). Given the structural similarities between various UFA-producing enzymes and FAD2, further characterization of their N-terminus and protein half-life in transgenic plant and yeast cells could aid the design of a more stable enzyme, thereby improving UFA production.

When *S. cerevisiae* BY4741 was cultured under 30 °C, C16 fatty acids accounted for over 60% of its total fatty acid composition (He et al., 2018; Sec et al., 2015). In comparison, total C16 fatty acid only accounted for 9% at 72 h in BY4741-derived CARIC568 grown at 20 °C (Table 1). Combining the effects of PgFAD2 and RnELO2, these enzymes greatly contributed to the *in vivo* increase of the C18 fatty acid precursor level and stimulated PuA production. Regarding the genes introduced in the second round of integration, *PDCT*, *LPCAT*, and *DGAT2* are particularly important for enriching UFA in plants. A previous study revealed that castor RcPDCT and RcDGAT2 may work in concert to increase tri-ricinoleoyl glycerol levels in castor seeds while also generating nonricinoleate lipids for membrane biosynthesis (Demski et al., 2022). As illustrated in Fig. 1A, plant LPCAT was also involved in this process by catalyzing both the forward reaction to synthesize PC and the reverse reaction to release acyl-CoA (Lager et al., 2013). Certain plant LPCAT was shown to have low activities with UFA groups in the forward reaction, but higher activity on common fatty acids (Arroyo-Caro et al., 2013; Lager et al., 2013), suggesting its role in recruiting specific precursor acyl-CoA into PC for UFA synthesis.

S. cerevisiae's physiology and cellular processes rely heavily on PL. For example, PC, the most abundant phospholipid in *S. cerevisiae* membranes, contributes to the maintenance of membrane integrity, fluidity, and stability (Hein and Hayen, 2012). Therefore, ideally, the introduced PuA-producing pathway should cause as little disturbance as possible to the yeast's native PL species. However, as shown in Fig. 5D, substantial up-regulation was observed across major PL species following PuA accumulation capability. Certain important branching points exist in PL biosynthesis that may control the acyl-chain species. For example, yeast PE-producing enzyme (EPT1) showed the highest activity towards di-unsaturated DAG species as substrates and yeast

PC-producing enzyme (CPT1) favored C32:2 substrates (Boumann et al., 2004). A previous study on human CDP-diacylglycerol synthases (CDS) also revealed that this key enzyme, catalyzing the formation of CDP-diacylglycerol, exhibited acyl-chain specificities for its lipid substrate (D'Souza et al., 2014). Although little information is known concerning baker's yeast native lipid synthetic enzymes' selectivity on conjugated PUFA, the polar lipidomic profile obtained in this study suggested substantial crosstalk between PuA and yeast major PL synthetic pathways.

On the other hand, the presence of PuA in yeast PL and its accompanied influence on cellular fitness may contribute to the design of novel rapid screening methods, targeting cells with higher PuA. Since screening by gas chromatography is relatively time-consuming and labor-intensive, previous studies have used UV spectral scans to detect the amount of conjugated dienes and trienes in bacterial isolates or pomegranate oils (Liu et al., 2012; Ülker et al., 2016). However, such methods still require the prior extraction of conjugated fatty acids. Alternatively, the membrane lipid composition of *S. cerevisiae* is known to affect strain survival under stress conditions (Henderson and Block, 2014). For instance, when *Arabidopsis FAD2* was expressed in *S. cerevisiae*, yeast cells acquired greater resistance to ethanol stress (Kajiwara et al., 1996). Expressing *FAD2* from the rubber tree (*Hevea brasiliensis*) increased *S. cerevisiae*'s susceptibility to oxidative stress, triggered by paraquat, tertbutyl hydroperoxide, and hydrogen peroxide-induced lipid peroxidation (Cipak et al., 2006). From a future perspective, it would be intriguing to examine how CARIC568 responds to these stress factors. These stress conditions could serve as selective or counter-selective measures to identify the strain with the highest PuA levels among the transformants produced by Ty retrotransposon-targeted random gene shuffling.

It should also be noted that given *S. cerevisiae*'s limited PuA accumulating capabilities (0.3–3.7%) observed in our previous study (Wang et al., 2021), for the second round of integration, we chose to screen pomegranate genes on yeast genome based on the bioconversion method. In the future, it would be interesting to conduct another round of Ty retrotransposon-targeted random gene shuffling of pomegranate acyl-editing and TAG assembly genes on CARIC568, with the approach described in Fig. 2. Given the presence of a complete pathway for PuA neosynthesis, a better combination of pomegranate genes in terms of *de novo* PuA production would be identified. In addition, considering the potential contribution of yeast native lipid biosynthesis to PuA accumulation, the genes encoding yeast native fatty acid synthesis and TAG assembly enzymes in CARIC568 were kept intact. However, a previous report suggested that isozyme competition might be a limiting factor in the engineering of UFA production in heterologous hosts (van Erp et al., 2015). Similarly, in this study, yeast native enzymes may also compete with heterologous enzymes and preferentially integrate fatty acids other than PuA into the glycerol backbone of the TAG. Therefore, replacing them with equivalent heterologous genes in future studies may further enhance PuA levels in yeast lipids.

5. Conclusions

In this study, genes potentially contributing to plant-derived PuA synthesis were directly integrated and shuffled in the *S. cerevisiae* genome. High throughput screening led to the identification of a recombinant strain capable of accumulating 26.7% of total fatty acids as PuA without LA precursor feeding. In shake flask cultivation, the PuA titer reached 425 mg/L. PuA comprised over 22% of total fatty acids in the TAG fraction of yeast single-cell oil, a significant

increase compared to transgenic *A. thaliana* and *B. napus*. Subsequent analysis revealed significant lipidome changes due to PuA synthesis. Based on these results, the PuA level in this PuA-enriched yeast platform could be further enhanced by iterative integration using the same workflow.

Author Statement

JW contributed to the conceptualization, methodology, investigation, formal analysis, visualization, and writing- original draft preparation. GC contributed to the conceptualization, supervision, resources and funding acquisition, reviewing, and editing.

Declaration of competing interest

A provisional application has been filed (US 63/636,208), and JW and GC are listed as inventors.

Data availability

Data needed to evaluate the conclusions in the paper are present in the paper and/or the supplementary materials. All sequences for the construction of CRISPR-Cas9 and the assembly of pomegranate genes used in this work can be found in the supplementary information. All accession codes are provided.

Acknowledgment

We acknowledge the support provided by the Natural Sciences and Engineering Research Council of Canada Discovery Grant (RGPIN-2016-05926, RGPIN-2023-04199), the Natural Sciences and Engineering Research Council of Canada Alliance grant (ALLRP 561166 - 20), the

Canada Research Chairs Program, Alberta Innovates (2019F111R), Canadian Poultry Research Council (AMN122), Cargill/Diamond V, Results Driven Agriculture Research (2019F111R; 2024F2341R), Alberta Canola Producers Commission (2024F2341R), Western Grains Research Foundation (2024F2341R), Canada Foundation for Innovation-John R. Evans Leaders Fund (Project number 41867) and Research Capacity Program of Alberta (RCP-22-023-SEG). We sincerely thank Dr. Ruth Welti and Ms. Mary Roth of Kansas State University for the lipidomic analysis. Instrument acquisition and lipidomic method development in the Kansas Lipidomics Research Center were supported by the National Science Foundation (including support from the Major Research Instrumentation program; most recent award DBI-1726527), K-IDeA Networks of Biomedical Research Excellence (INBRE) of National Institute of Health (P20GM103418), USDA National Institute of Food and Agriculture (Hatch/Multi-State project 1013013), and Kansas State University.

References

Andre, C., Kim, S.W., Yu, X.-H., Shanklin, J., 2013. Fusing catalase to an alkane-producing enzyme maintains enzymatic activity by converting the inhibitory byproduct H_2O_2 to the cosubstrate O_2. Proc. Natl. Acad. Sci. 110, 3191–3196. https://doi.org/10.1073/pnas.1218769110

Arroyo-Caro, J.M., Chileh, T., Alonso, D.L., García-Maroto, F., 2013. Molecular characterization of a lysophosphatidylcholine acyltransferase gene belonging to the MBOAT family in *Ricinus communis* L. Lipids 48, 663–674. https://doi.org/10.1007/s11745-013-3797-z

Bao, Z., Xiao, H., Liang, J., Zhang, L., Xiong, X., Sun, N., Si, T., Zhao, H., 2015. Homology-integrated CRISPR–Cas (HI-CRISPR) system for one-step multigene disruption in *Saccharomyces cerevisiae*. ACS Synth. Biol. 4, 585–594. https://doi.org/10.1021/sb500255k

Baumann, H.A., de Kruijff, B., Heck, A.J.R., de Kroon, A.I.P.M., 2004. The selective utilization of substrates *in vivo* by the phosphatidylethanolamine and phosphatidylcholine biosynthetic enzymes Ept1p and Cpt1p in yeast. FEBS Lett. 569, 173–177. https://doi.org/10.1016/j.febslet.2004.05.043

Browse, J.A., Slack, C.R., 1981. Catalase stimulates linoleate desaturase activity in microsomes from developing linseed cotyledons. FEBS Lett. 131, 111–114. https://doi.org/10.1016/0014-5793(81)80899-X

Cahoon, E.B., Li-Beisson, Y., 2020. Plant unusual fatty acids: learning from the less common. Curr. Opin. Plant Biol. 55, 66–73. https://doi.org/10.1016/j.pbi.2020.03.007

Cerone, M., Smith, T.K., 2022. Desaturases: Structural and mechanistic insights into the biosynthesis of unsaturated fatty acids. Iubmb Life 74, 1036–1051. https://doi.org/10.1002/iub.2671

Chen, G., Harwood, J.L., Lemieux, M.J., Stone, S.J., Weselake, R.J., 2022. Acyl-CoA:diacylglycerol acyltransferase: Properties, physiological roles, metabolic engineering and intentional control. Prog. Lipid Res. 88, 101181. https://doi.org/10.1016/j.plipres.2022.101181

Cirpak, A., Hasslacher, M., Tehlivets, O., Collinson, E.J., Zivkovic, M., Matijevic, T., Wonisch, W., Waeg, G., Dawes, I.W., Zarkovic, N., Kohlwein, S.D., 2006. *Saccharomyces cerevisiae* strain expressing a plant fatty acid desaturase produces polyunsaturated fatty

acids and is susceptible to oxidative stress induced by lipid peroxidation. Free Radic. Biol. Med. 40, 897–906. https://doi.org/10.1016/j.freeradbiomed.2005.10.039

Curcio, M.J., Lutz, S., Lesage, P., 2015. The Ty1 LTR-retrotransposon of budding yeast, *Saccharomyces cerevisiae*. Microbiol. Spectr. 3, 3.2.19. https://doi.org/10.1128/microbiolspec.MDNA3-0053-2014

Demski, K., Jeppson, S., Stymne, S., Lager, I., 2022. Phosphatidylcholine:diacylglycerol cholinephosphotransferase's unique regulation of castor bean oil quality. Plant Physiol. 189, 2001–2014. https://doi.org/10.1093/plphys/kiac209

D'Souza, K., Kim, Y.J., Balla, T., Epand, R.M., 2014. Distinct properties of the two isoforms of CDP-diacylglycerol synthase. Biochemistry 53, 7358–7367. https://doi.org/10.1021/bi501250m

Fadavi, A., Barzegar, M., Hossein Azizi, M., 2006. Determination of fatty acids and total lipid content in oilseed of 25 pomegranates varieties grown in Iran. J. Food Compos. Anal., Biodiversity and nutrition: a common path 19, 676–680. https://doi.org/10.1016/j.jfca.2004.09.002

Garaiova, M., Mietkiewska, E., Weselake, R.J., Holic, R., 2017. Metabolic engineering of *Schizosaccharomyces pombe* to produce punicic acid, a conjugated fatty acid with nutraceutic properties. Appl. Microbiol. Biotechnol. 101, 7913–7922. https://doi.org/10.1007/s00253-017-8498-8

Gietz, R.D., Schiestl, R.H., 2007. Frozen competent yeast cells that can be transformed with high efficiency using the LiAc/SS carrier DNA/PEG method. Nat. Protoc. 2, 1–4. https://doi.org/10.1038/nprot.2007.17

He, Q., Yang, Y., Yang, S., Donohoe, B.S., Van Wychen, S., Zhang, M., Himmel, M.E., Knoshaug, E.P., 2018. Oleaginicity of the yeast strain *Saccharomyces cerevisiae* D5A. Biotechnol. Biofuels 11, 258. https://doi.org/10.1186/s13068-018-1256-z

Hein, E.-M., Hayen, H., 2012. Comparative lipidomic profiling of *S. cerevisiae* and four other hemiascomycetous yeasts. Metabolites 2, 254–267. https://doi.org/10.3390/metabo2010254

Henderson, C.M., Block, D.E., 2014. Examining the role of membrane lipid composition in determining the ethanol tolerance of *Saccharomyces cerevisiae*. Appl. Environ. Microbiol. 80, 2966–2972. https://doi.org/10.1128/AEM.04151-13

Idris, R., Xu, Y., Caldo, K.M.P., Singer, S.D., Field, C.J., Weselake, R.J., Chen, G., 2018. Bioactivity and biotechnological production of punicic acid. Appl. Microbiol. Biotechnol. 102, 3537–3549. https://doi.org/10.1007/s00253-018-8883-y

Iwabuchi, M., Kohno-Murase, J., Imamura, J., 2003. Delta 12-oleate desaturase-related enzymes associated with formation of conjugated trans-delta 11, cis-delta 13 double bonds. J. Biol. Chem. 278, 4603–4610. https://doi.org/10.1074/jbc.M210748200

Kajiwara, S., Shirai, A., Fujii, T., Toguri, T., Nakamura, K., Ohtaguchi, K., 1996. Polyunsaturated fatty acid biosynthesis in *Saccharomyces cerevisiae*: expression of ethanol tolerance and the FAD2 gene from *Arabidopsis thaliana*. Appl. Environ. Microbiol. 62, 4309–4313. https://doi.org/10.1128/aem.62.12.4309-4313.1996

Kamisaka, Y., Noda, N., Tomita, N., Kimura, K., Kodaki, T., Hosaka, K., 2006. Identification of genes affecting lipid content using transposon mutagenesis in *Saccharomyces cerevisiae*. Biosci. Biotechnol. Biochem. 70, 646–653. https://doi.org/10.1271/bbb.70.646

Karim, A.S., Curran, K.A., Alper, H.S., 2013. Characterization of plasmid burden and copy number in *Saccharomyces cerevisiae* for optimization of metabolic engineering applications. FEMS Yeast Res. 13, 107–116. https://doi.org/10.1111/1567-1364.12016

Kato, H., Matsuda, F., Yamada, R., Nagata, K., Shirai, T., Hasunuma, T., Kondo, A., 2013. Cocktail δ-integration of xylose assimilation genes for efficient ethanol production from xylose in *Saccharomyces cerevisiae*. J. Biosci. Bioeng. 116, 333–336. https://doi.org/10.1016/j.jbiosc.2013.03.020

Kaufman, M., Wiesman, Z., 2007. Pomegranate oil analysis with emphasis on MALDI-TOF/MS triacylglycerol fingerprinting. J. Agric. Food Chem. 55, 10405–10413. https://doi.org/10.1021/jf072741q

Khoddami, A., Man, Y.B.C., Roberts, T.H., 2014. Physico-chemical properties and fatty acid profile of seed oils from pomegranate (*Punica granatum* L.) extracted by cold pressing. Eur. J. Lipid Sci. Technol. 116, 553–562. https://doi.org/10.1002/ejlt.201300416

Khuu, N., Gidda, S., Shockey, J.M., Dyer, J.M., Mullen, R.T., 2011. The N termini of *Brassica* and tung omega-3 fatty acid desaturases mediate proteasome-dependent protein degradation in plant cells. Plant Signal. Behav. 6, 422–425. https://doi.org/10.4161/psb.6.3.14522

Lager, I., Yilmaz, J.L., Zhou, X.-R., Jasieniecka, K., Kazachkov, M., Wang, P., Zou, J., Weselake, R., Smith, M.A., Bayon, S., Dyer, J.M., Shockey, J.M., Heinz, E., Green, A., Banas, A., Stymne, S., 2013. Plant acyl-CoA:lysophosphatidylcholine acyltransferases (LPCATs) have different specificities in their forward and reverse reactions. J. Biol. Chem. 288, 36902–36914. https://doi.org/10.1074/jbc.M113.521815

Lansky, E.P., Newman, R.A., 2007. *Punica granatum* (pomegranate) and its potential for prevention and treatment of inflammation and cancer. J. Ethnopharmacol. 109, 177–206. https://doi.org/10.1016/j.jep.2006.09.006

Lian, J., Jin, R., Zhao, H., 2016. Construction of plasmids with tunable copy numbers in *Saccharomyces cerevisiae* and their applications in pathway optimization and multiplex genome integration: Plasmid Copy Number Engineering. Biotechnol. Bioeng. 113, 2462–2473. https://doi.org/10.1002/bit.26004

Liao, X., Li, H., Chen, Y., Cao, Y., 2012. Method for screening of bacterial strains biosynthesizing specific conjugated linoleic acid isomers. J. Agric. Food Chem. 60, 9705–9710. https://doi.org/10.1021/jf3032843

Luddy, F.E., Barford, R.A., Herb, S.F., Magidman, P., Riemenschneider, R.W., 1964. Pancreatic lipase hydrolysis of triglycerides by a semimicro technique. J. Am. Oil Chem. Soc. 41, 693–696. https://doi.org/10.1007/BF02661412

Luo, X., Li, H., Wu, Z., Yao, W., Zhao, P., Cao, D., Yu, H., Li, K., Poudel, K., Zhao, D., Zhang, F., Xia, X., Chen, L., Wang, Q., Jing, D., Cao, S., 2020. The pomegranate (*Punica granatum* L.) draft genome dissects genetic divergence between soft□ and hard□seeded cultivars. Plant Biotechnol. J. 18, 955–968. https://doi.org/10.1111/pbi.13260

Mietkiewska, E., Miles, R., Wickramarathna, A., Sahibollah, A.F., Greer, M.S., Chen, G., Weselake, R.J., 2014. Combined transgenic expression of *Punica granatum* conjugase (FADX) and FAD2 desaturase in high linoleic acid *Arabidopsis thaliana* mutant leads to increased accumulation of punicic acid. Planta 240, 575–583. https://doi.org/10.1007/s00425-014-2109-z

Napier, J.A., 2007. The production of unusual fatty acids in transgenic plants. Annu. Rev. Plant Biol. 58, 295–319. https://doi.org/10.1146/annurev.arplant.58.032806.103811

Pan, X., Siloto, R.M.P., Wickramarathna, A.D., Mietkiewska, E., Weselake, R.J., 2013. Identification of a pair of phospholipid:diacylglycerol acyltransferases from developing flax (*Linum usitatissimum* L.) seed catalyzing the selective production of trilinolenin. J. Biol. Chem. 288, 24173–24188. https://doi.org/10.1074/jbc.M113.475699

Paul, A., Radhakrishnan, M., 2020. Pomegranate seed oil in food industry: Extraction, characterization, and applications. Trends Food Sci. Technol. 105, 273–283. https://doi.org/10.1016/j.tifs.2020.09.014

Salimon, J., Abdullah, B.M., Salih, N., 2011. Hydrolysis optimization and characterization study of preparing fatty acids from *Jatropha curcas* seed oil. Chem. Cent. J. 5, 67. https://doi.org/10.1186/1752-153X-5-67

Sandager, L., Gustavsson, M.H., Ståhl, U., Dahlqvist, A., Wiberg, E., Banas, A., Lenman, M., Ronne, H., Stymne, S., 2002. Storage lipid synthesis is non-essential in yeast. J. Biol. Chem. 277, 6478–6482. https://doi.org/10.1074/jbc.M109109200

Sec, P., Garaiova, M., Gajdos, P., Certik, M., Griac, P., Hapala, I., Holic, R., 2015. Baker's yeast deficient in storage lipid synthesis uses cis-vaccenic acid to reduce unsaturated fatty acid toxicity. Lipids 50, 621–630. https://doi.org/10.1007/s11745-015-4022-z

Seip, J., Jackson, R., He, H., Zhu, Q., Hong, S.-P., 2013. Snf1 is a regulator of lipid accumulation in *Yarrowia lipolytica*. Appl. Environ. Microbiol. 79, 7360–7370. https://doi.org/10.1128/AEM.02079-13

Shi, S., Liang, Y., Zhang, M.M., Ang, E.L., Zhao, H., 2016. A highly efficient single-step, markerless strategy for multi-copy chromosomal integration of large biochemical

pathways in *Saccharomyces cerevisiae*. Metab. Eng. 33, 19–27. https://doi.org/10.1016/j.ymben.2015.10.011

Shockey, J., Rinehart, T., Chen, Y., Yangdong, W., Zhiyong, Z., Lisong, H., 2016. Tung (*Vernicia fordii* and *Vernicia montana*), in: McKeon, T.A., Hayes, D.G., Hildebrand, D.F., Weselake, R.J. (Eds.), Industrial Oil Crops. AOCS Press, pp. 243–273. https://doi.org/10.1016/B978-1-893997-98-1.00010-5

Ülker, S., Placidi, C., Point, V., Gadenne, B., Serveau-Avesque, C., Canaan, S., Carrière, F., Cavalier, J.-F., 2016. New lipase assay using Pomegranate oil coating in microtiter plates. Biochimie 120, 110–118. https://doi.org/10.1016/j.biochi.2015.09.004

Urbanikova, V., Park, Y.-K., Krajciova, D., Tachekort, M., Certik, M., Grigoras, I., Holic, R., Nicaud, J.-M., Gajdos, P., 2023. *Yarrowia lipolytica* as a platform for punicic acid production. Int. J. Mol. Sci. 24, 8823. https://doi.org/10.3390/ijms24108823

Usaite, R., Jewett, M.C., Oliveira, A.P., Yates, J.R., Olsson, L., Nielsen, J., 2009. Reconstruction of the yeast Snf1 kinase regulatory network reveals its role as a global energy regulator. Mol. Syst. Biol. 5, 319. https://doi.org/10.1038/msb.2009.67

van Erp, H., Shockey, J., Zhang, M., Adhikari, N.D., Browse, J., 2015. Reducing isozyme competition increases target fatty acid accumulation in seed triacylglycerols of transgenic *Arabidopsis*. Plant Physiol. 168, 36–46. https://doi.org/10.1104/pp.114.254110

Vikbjerg, A.F., Mu, H., Xu, X., 2006. Elucidation of acyl migration during lipase catalyzed production of structured phospholipids. J. Am. Oil Chem. Soc. 83, 609–614. https://doi.org/10.1007/s11746-006-1246-3

Wang, J., Xu, Y., Holic, R., Yu, X., Singer, S.D., Chen, G., 2021. Improving the production of punicic acid in baker's yeast by engineering genes in acyl channeling processes and

adjusting precursor supply. J. Agric. Food Chem. 69, 9616–9624. https://doi.org/10.1021/acs.jafc.1c03256

Xu, Y., Caldo, K.M.P., Falarz, L., Jayawardhane, K., Chen, G., 2020a. Kinetic improvement of an algal diacylglycerol acyltransferase 1 via fusion with an acyl□CoA binding protein. Plant J. 102, 856–871. https://doi.org/10.1111/tpj.14708

Xu, Y., Mietkiewska, E., Shah, S., Weselake, R.J., Chen, G., 2020b. Punicic acid production in *Brassica napus*. Metab. Eng. 62, 20–29. https://doi.org/10.1016/j.ymben.2020.08.011

Yazawa, H., Iwahashi, H., Kamisaka, Y., Kimura, K., Uemura, H., 2010. Improvement of polyunsaturated fatty acids synthesis by the coexpression of CYB5 with desaturase genes in *Saccharomyces cerevisiae*. Appl. Microbiol. Biotechnol. 87, 2185–2193. https://doi.org/10.1007/s00253-010-2679-z

Figure captions

Fig. 1. TAG and UFA synthetic pathways and functional analysis of enzyme in yeast strain H1246. (A) Rewiring the lipid biosynthetic pathway in *S. cerevisiae* to produce PuA. Yellow ellipses indicate *S. cerevisiae* native enzymes. Green ellipses indicate enzymes from *P. granatum*. Blue ellipses indicate enzymes from other sources. DGAT/DGA1, acyl-CoA: diacylglycerol acyltransferase; GPAT/SCT1/GPT2, glycerol-3-phosphate acyltransferase; LACS/FAA, long-chain acyl-CoA synthetase; LPAT/SLC1, lysophosphatidic acid acyltransferase; LPC, lysophosphatidylcholine; LPCAT, lysophosphatidylcholine acyltransferase; PAP/APP1/PAH1, phosphatidate phosphatase; PC, phosphatidylcholine; PDAT/LRO1, phospholipid: diacylglycerol acyltransferase; PDCT, phosphatidylcholine: diacylglycerol cholinephosphotransferase; PLA2, phospholipase A2; ACC1, acetyl-CoA

carboxylase; FAS, fatty acid synthase; OLE1, acyl-CoA desaturase; ELO, fatty acid elongase; LOA1, lysophosphatidic acid: oleoyl-CoA acyltransferase; DGK1, diacylglycerol kinase; CDS1, phosphatidate cytidylyltransferase; EPT1, choline/ethanolamine phosphotransferase; PIS1, CDP-diacylglycerol--inositol 3-phosphatidyltransferase; PSD, phosphatidylserine decarboxylase; CPT, cholinephosphotransferase; PLC, phospholipase C; ALE1, lysophospholipid acyltransferase; FADX, bifunctional fatty acid conjugase/Delta(12)-oleate desaturase; FAD2, delta(12)-fatty-acid desaturase; PI, phosphatidylinositol; PE, phosphatidylethanolamine; CHO1, CDP-diacylglycerol-serine O-phosphatidyltransferase; PS, phosphatidylserine. Made with biorender.com. (B, C) Functional complementation assay in yeast strain H1246 without/with pomegranate oil hydrolysate. Lane 1-9, pomegranate oil, empty vector control, PgDGAT1, PgDGAT2a, PgDGAT2b, PgDGAT2c, PgPDAT.a, PgPDAT.b, PgPDAT.c respectively. (D) Fatty acid profiles of recombinant H1246 strains expressing different TAG assembly genes in the absence or presence of pomegranate oil hydrolysate. (E) PuA level in yeast strains transformed with various PgFADX protein fusions. Data represents mean ± SD of triplicates.

Fig. 2. Workflow design of the Ty retrotransposon-targeted random gene shuffling. (A) Schematic diagram depicting the screening procedure for Ty retrotransposon-targeted random gene shuffling by CRISPR-Cas9. (B) Schematic diagram of donor DNA design for integration into yeast Ty retrotransposons. Made with biorender.com.

Fig. 3. PuA production in *S. cerevisiae* strains constructed by Ty retrotransposon-targeted random gene shuffling. (A, C, E) Three-dimensional scatter plots of the results from round 1, round 2, and round 3 CRISPR-Cas9-assisted random integration, respectively. Each red dot

represents an individual yeast transformant. The yeast transformant's PuA content (represented by the percentage of PuA in total fatty acids, Z-axis), PuA amount (represented by the integrated area of PuA's peak, Y-axis), and neutral lipid level (represented by the Nile red fluorescence, X-axis) are shown. (B, D, F) Fatty acid composition and PuA production of CARIA266, CARIB650, and CARIC568 at different incubation times under different culturing temperatures. Data represents mean ± SD of triplicates.

Fig. 4. Growth condition optimization and the relative content of PuA in TAG and PL. (A, B) Three-dimensional surface plot of PuA content's response to carbon source level, and initial pH or initial OD_{600}. (C) Fatty acid composition of TAG. (D) Fatty acid composition of PL. (E) Fatty acid composition at the *sn*-2 position of TAG. (F) Fatty acid composition at the *sn*-1 position of PL. (G) The relative content of fatty acid at the *sn*-1/3 positions of TAG. (H) The relative content of fatty acid at the *sn*-2 position of PL. Data represents mean ± SD of triplicates.

Fig. 5. Yeast lipidomes containing PuA with or without LA feeding. (A) Heatmap of top-ranking SFA-containing TAG. (B) Heatmap of top-ranking MFA-containing TAG. (C) Heatmap of top-ranking PUFA-containing TAG. (D) Heatmap of top-ranking PL species. The levels of single lipid species are presented on a color scale ranging from black (low values) to yellow (high values), as described in the legend. (E-H) Volcano plots showing log2 (fold change) and -log10 (p values) of molecular lipid species comparing CARIA266+LA vs CARIA266, CARIB650+LA vs CARIA266+LA, CARIC568 vs CARIB650+LA, and CARIC568 vs CARIA266, respectively. Red or blue dots indicate up- or down-regulated lipid species, respectively, with a fold change >1.5 and p-value < 0.05.

Table 1. Fatty acid profile and PuA production of CARIC568 over a 6-day growth period in the optimized medium.

	Fatty acid content (% of total fatty acids)						PuA titer
	C16:0	**C16:1**	**C18:0**	**C18:1**	**C18:2**	**PuA**	**(mg/L)**
24h	6.5 ± 0.1	15.4 ± 1.2	13.3 ± 0.4	31.0 ± 1.0	26.4 ± 0.2	7.3 ± 0.4	26 ± 10
48h	2.8 ± 0.2	9.8 ± 0.4	13.0 ± 0.2	27.2 ± 0.2	31.4 ± 0.5	15.8 ± 0.7	180 ± 48
72h	1.4 ± 0.1	7.6 ± 0.3	11.0 ± 0.5	27.4 ± 0.3	31.1 ± 0.4	21.5 ± 0.1	272 ± 36
96h	0.9 ± 0.04	7.0 ± 0.5	8.8 ± 0.6	26.4 ± 0.9	31.8 ± 0.7	25.1 ± 0.4	331 ± 32
120h	0.8 ± 0.1	7.0 ± 0.9	7.3 ± 0.6	26.5 ± 0.9	31.7 ± 0.3	26.7 ± 1.0	425 ± 33
144h	0.6 ± 0.04	6.8 ± 0.8	6.8 ± 0.2	26.9 ± 0.9	32.3 ± 0.4	26.6 ± 1.2	380 ± 59

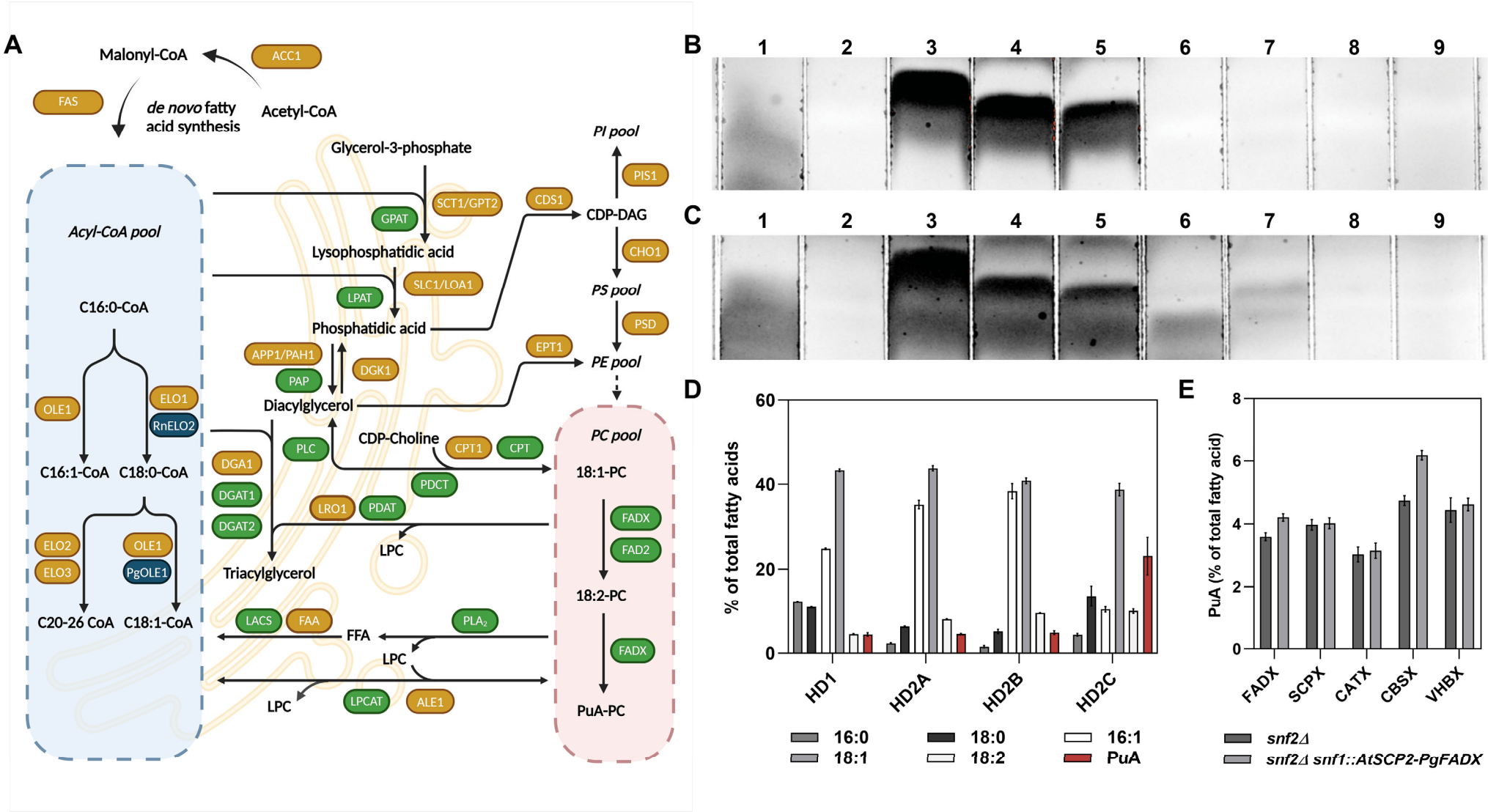
A
Malonyl-CoA
ACC1
FAS
de novo fatty acid synthesis
Acetyl-CoA
Glycerol-3-phosphate
Acyl-CoA pool
C16:0-CoA
OLE1
ELO1
RnELO2
C16:1-CoA
C18:0-CoA
ELO2
ELO3
OLE1
PgOLE1
C20-26 CoA
C18:1-CoA
GPAT
SCT1/GPT2
Lysophosphatidic acid
LPAT
SLC1/LOA1
Phosphatidic acid
APP1/PAH1
PAP
DGK1
Diacylglycerol
DGA1
DGAT1
DGAT2
Triacylglycerol
PLC
CDP-Choline
CPT1
CPT
PDCT
LRO1
PDAT
LPC
LACS
FAA
FFA
PLA2
LPC
LPC
LPCAT
ALE1
CDS1
CDP-DAG
PI pool
PIS1
CHO1
PS pool
PSD
EPT1
PE pool
PC pool
18:1-PC
FADX
FAD2
18:2-PC
FADX
PuA-PC
B
1 2 3 4 5 6 7 8 9
C
1 2 3 4 5 6 7 8 9
D
% of total fatty acids
60
40
20
0
HD1
HD2A
HD2B
HD2C
16:0
18:1
18:0
18:2
16:1
PuA
E
PuA (% of total fatty acid)
8
6
4
2
0
FADX
SCPX
CATX
CBSX
VHBX
snf2Δ
snf2Δ snf1::AtSCP2-PgFADX

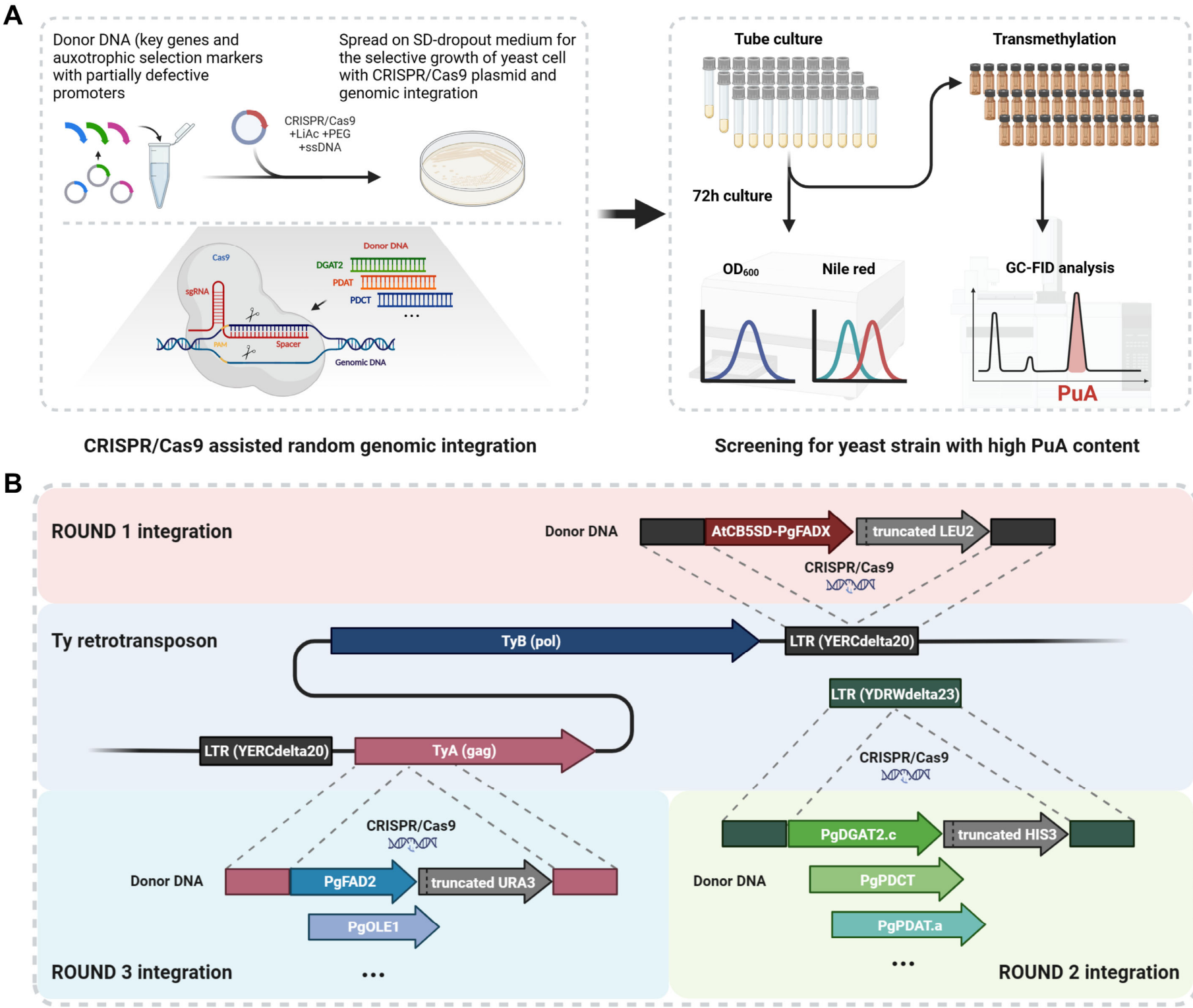
A
Donor DNA (key genes and auxotrophic selection markers with partially defective promoters
Spread on SD-dropout medium for the selective growth of yeast cell with CRISPR/Cas9 plasmid and genomic integration
CRISPR/Cas9
+LiAc +PEG
+ssDNA
Cas9
sgRNA
Donor DNA
DGAT2
PDAT
PDCT
PAM
Spacer
Genomic DNA
CRISPR/Cas9 assisted random genomic integration
Tube culture
Transmethylation
72h culture
OD600
Nile red
GC-FID analysis
PuA
Screening for yeast strain with high PuA content
B
ROUND 1 integration
Donor DNA
AtCB5SD-PgFADX
truncated LEU2
CRISPR/Cas9
Ty retrotransposon
TyB (pol)
LTR (YERCdelta20)
LTR (YDRWdelta23)
LTR (YERCdelta20)
TyA (gag)
CRISPR/Cas9
CRISPR/Cas9
Donor DNA
PgFAD2
truncated URA3
PgOLE1
ROUND 3 integration
PgDGAT2.c
truncated HIS3
Donor DNA
PgPDCT
PgPDAT.a
ROUND 2 integration

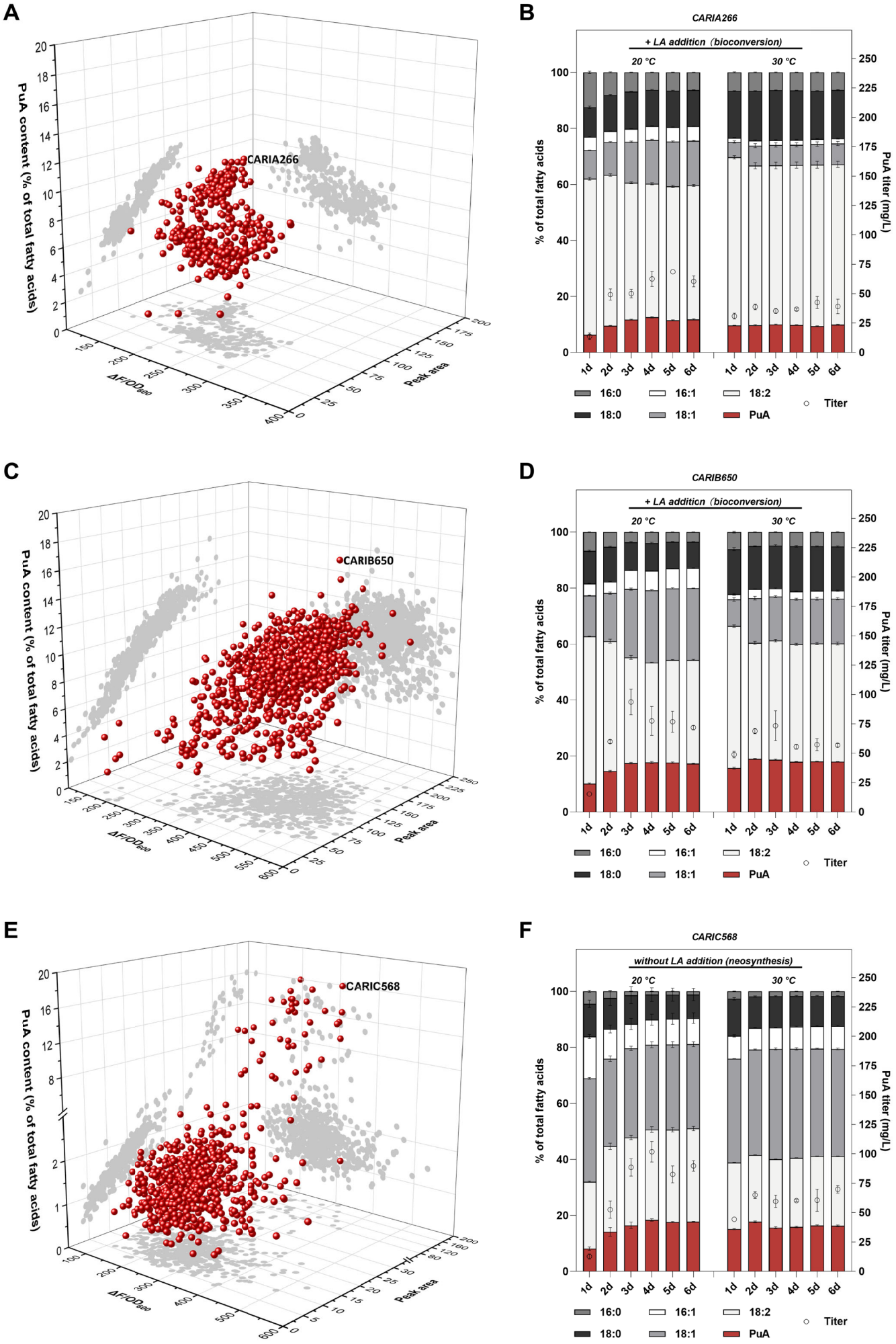
A
PuA content (% of total fatty acids)
CARIA266
ΔFIOD600
Peak area
B
CARIA266
+ LA addition (bioconversion)
20 °C
30 °C
% of total fatty acids
PuA titer (mg/L)
1d
2d
3d
4d
5d
6d
16:0
16:1
18:2
18:0
18:1
PuA
Titer
C
PuA content (% of total fatty acids)
CARIB650
ΔFIOD600
Peak area
D
CARIB650
+ LA addition (bioconversion)
20 °C
30 °C
% of total fatty acids
PuA titer (mg/L)
16:0
16:1
18:2
18:0
18:1
PuA
Titer
E
PuA content (% of total fatty acids)
CARIC568
ΔFIOD600
Peak area
F
CARIC568
without LA addition (neosynthesis)
20 °C
30 °C
% of total fatty acids
PuA titer (mg/L)
16:0
16:1
18:2
18:0
18:1
PuA
Titer

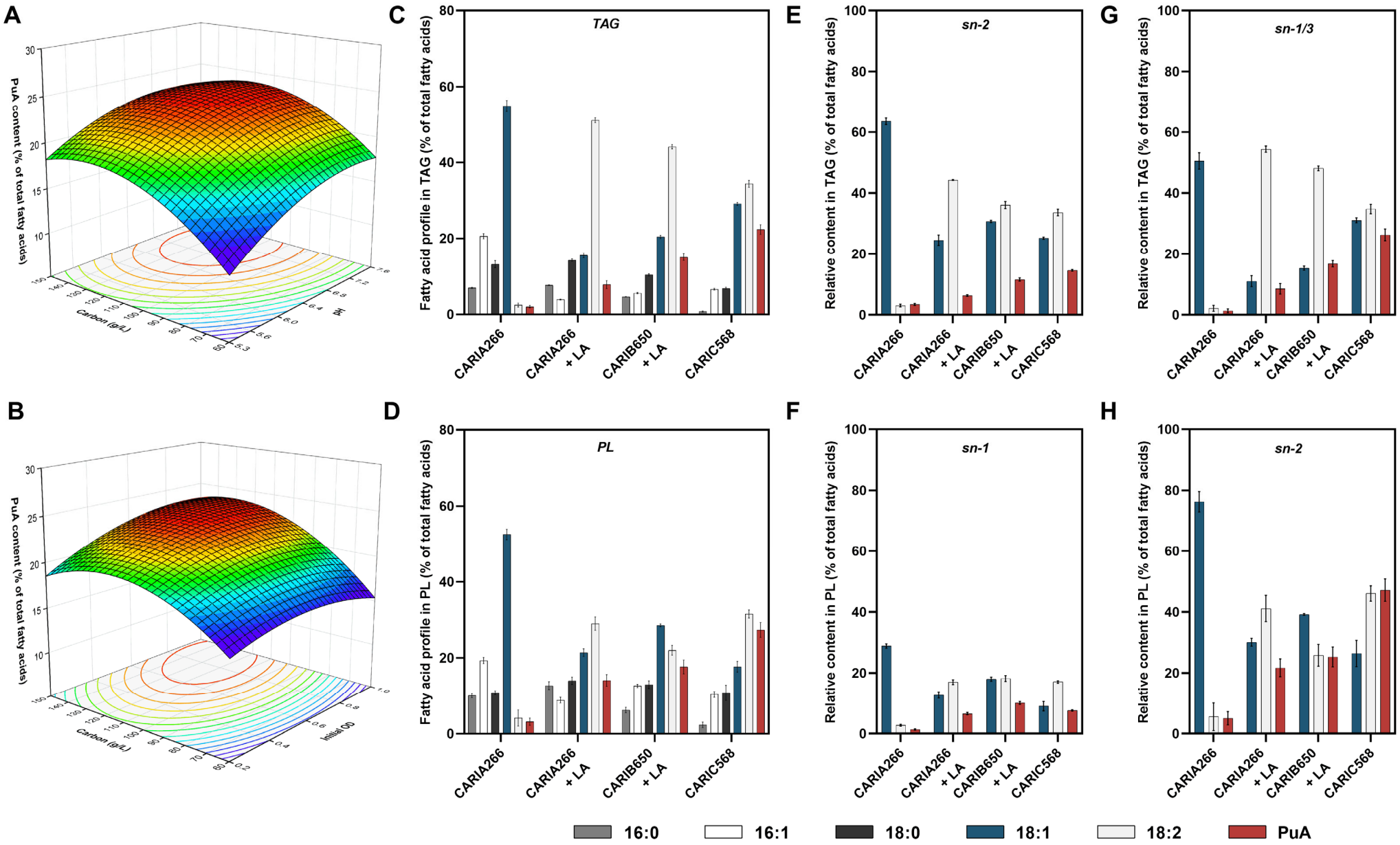
A
B
C
D
E
F
G
H
PuA content (% of total fatty acids)
Carbon (g/L)
pH
Initial OD
TAG
PL
sn-2
sn-1
sn-1/3
Fatty acid profile in TAG (% of total fatty acids)
Fatty acid profile in PL (% of total fatty acids)
Relative content in TAG (% of total fatty acids)
Relative content in PL (% of total fatty acids)
CARIA266
CARIA266 + LA
CARIB650 + LA
CARIC568
16:0
16:1
18:0
18:1
18:2
PuA

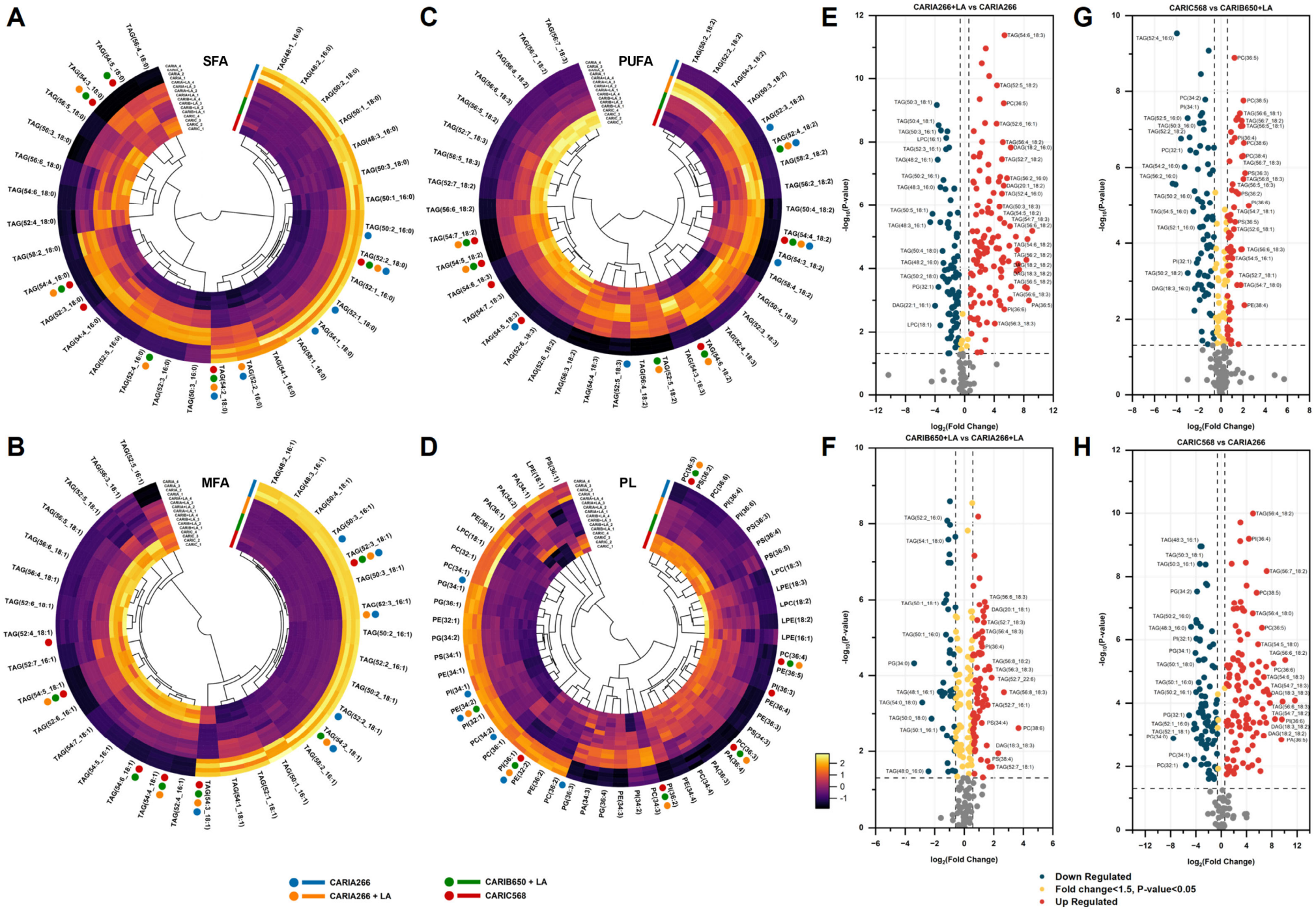
A
SFA
B
MFA
C
PUFA
D
PL
E
CARIA266+LA vs CARIA266
F
CARIB650+LA vs CARIA266+LA
G
CARIC568 vs CARIB650+LA
H
CARIC568 vs CARIA266
-log10(P-value)
log2(Fold Change)
CARIA266
CARIA266 + LA
CARIB650 + LA
CARIC568
Down Regulated
Fold change<1.5, P-value<0.05
Up Regulated